Investigation of Light Parameters on Image Quality in Optical Coherence Tomography

Boka Fikadu Banti (boka@aims.ac.za)
African Institute for Mathematical Sciences (AIMS)

Supervised by: Dr. Pieter Neethling and Dr. Gurthwin Bosman
Laser Research Institute, University of Stellenbosch, South Africa

14 May 2020

Submitted in partial fulfillment of a structured masters degree at AIMS South Africa

Abstract

In this work the quality of an image in optical coherence tomography was investigated. The study results show that there are highly significant difference between ultrasound and optical coherence tomography to produce an image with different wave. To understand this we studied the basic principle of optical coherence tomography in Michelson interferometer using monochromatic and broadband sources. The measurements of time domain and spectral domain, which exist at detectors, will be briefly described from a sample glass.

keywords : Optical coherence tomography, Time domain, Spectral domain, and light source.

Declaration

I, the undersigned, hereby declare that the work contained in this research project is my original work, and that any work done by others or by myself previously has been acknowledged and referenced accordingly.

Boka Fikadu Banti, 14 May 2020

Contents

1. Introduction

Optical coherence tomography (OCT) was first introduced in 1991 by Professor Huang et al., where they have found many uses outside of ophthalmology, as OCT has been used to image certain non-transparent tissues (Huang et al., 1991). OCT is an optical instrument that produces a cross sectional image of biological tissue within less than 10 microns axial resolution using light waves.

Moreover, OCT is a technique currently employed in medicine and biology capable of producing high resolution, and cross-sectional images of biological tissues. This includes transparent tissues such as, the eyes, and highly scattering tissues, like skin (Fujimoto et al., 2000). OCT has very similar applications to ultrasound imaging, but instead of using time of flight measurements OCT utilizes the interference nature of light waves to produce coherence gating. One of the most important components of OCT is that there is no ionizing radiation and it is not not necessary to prepare a sample.

Additionally, OCT is comparatively safe when compared with another techniques that use X-rays, because it uses light sources without ionizing radiation being involved. Further, having the advantage of being anoninvasive (in vivo) technique, OCT systems show great potential in the future of medical diagnostics. Today, scanning of retinas to reveal defects in underlying tissue is the area of most success for OCT, and stand alone units are being sold commercially (Pircher et al., 2003).

The OCT technique is limited to imaging size of up to 1 mm below the surface of biological tissue. OCT is a specifically good at scanning the retina. As the, retina is easily accessible to external light, making OCT specially good for diagnosine disorders. The light enters the eyes and the retina converts them into electric signals and passes then to the brain for the forming or reconstructon images. The major component of the retina are optics disk, macula, and blood vessels. By using OCT it is easy to see ten different tissue layers inside of the retina.

The first applications of OCT for use in medicine was reported less than a decade ago. However, its roots lie in early work on white light interferometry, that led to the development of optical coherence domain reflectometry (OCDR), a one dimensional optical detection technique (Youngquist et al., 1987). OCDR was originally developed for detecting faults in defect optic fibers and optical network components, however its ability to probe the eye and other biological tissues was soon recognized (Schmitt, 1999).

OCT is a modern variant of a Michelson interferometer, which worked by removing one side of the reference mirror and replacing it by a sample glass, and to determine the image of the tissue using monochromatic sources and broadband sources. OCT is basically working as a time domain and spectral domain optical coherence tomography. In time domain optical coherence tomography the reference mirror must be moving for measuring depth analysis, however spectral domain optical coherence tomography is a Fourier transform analysis without moving the mirror.

In this essay we discuss the use of modern optical instruments, specifically for measurements using a Michelson interferometer. Additionally, we simulate the signal Fourier transforms of the materials and compare with the results of an image of sample.

1.1 Objective

The main objective of this project is to determine the images of OCT using low coherence interference. As a result, to determine time domain and spectral domain optical coherence tomography in broadband sources.

1.2 General Outline

In our essay we will explain the basic principles of OCT, so that an OCT system can be constructed in the Michelson interferometer experiment. We want to do a theoretical formulation of the expected results based on the basic physical phenomena center to OCT. This includes basic concepts from optics-like interference, coherence and light (matter) interactions, with an understanding of the technological parameters of OCT. We are going to see the simulation results of signal intensity using modern optics OCT (chapter 4). Before that, in chapter two we will look to explanations of the Fresnel equations, focusing on light incident perpendicular to the surface, and in chapter three we cover the explanation of the basic principle of OCT. We are going to focus on the OCT in setting up of Michelson interferometer techniques, where we will look to simulating some results from a practical experiment.

2. Literature Review

In this chapter we will explains and derived the mathematical law for: reflection, refraction, the Fresnel equation, reflectance and transmittance intensity, and coherence.

2.1 Reflection

Reflection occurs when there is a region of sharp refractive index mismatch.. The light is split into two when it reaches an interface between the media where some of the light is transmitted and some of is reflected. When light passes through the different media the velocity is not the same. Light travels faster in the medium with low refractive index when compared with the medium of high refractive index. The law of reflection states that the incident angle θ_i and reflected angle θ_r are equal, and the reflected and incident light are in the same plane (Hecht, 1998). Figure 2.1 shows the reflection of a ray of light.

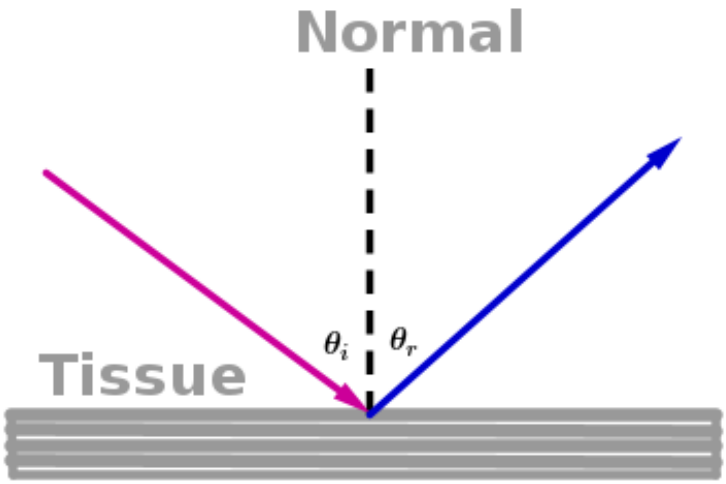

Figure 2.1: The reflection Light passing from one medium to another medium (Peatross and Ware, 2015)

According to figure 2.1 the angle of incidence θ_i is equal to the angle of reflection θ_r. Therefore the equation is given by

$$\theta_i = \theta_r \,. \tag{2.1.1}$$

2.2 Refraction

Light travels in different medium. During this travel the light bends in going from one medium to another medium, which is called refraction. Light rays coming from air that are not incident perpendicular to glass will be bend. Instead they are getting bend. Consider a glass slab and suppose a narrow beam of light is incident on one side. The beam of light is partially refracted, partially reflected, and can even

be partially absorbed by the object. The refracted ray is bent toward the normal when the light passes from a medium of low refractive index to one of high refractive index. However, if light travels from a material of high refractive index to one of low refractive index, it is bent away from the normal. When the incident light is perpendicular to the surface it does not change its direction. According to the law of refraction all of the incident ray, refracted ray and normal plane at the point of incident exist in the same plane.

$$\sin\theta_i = \sin\theta_r \,. \tag{2.2.1}$$

This law requires the use of the refractive index of a medium, which increases or decreases related to the speed of light in the medium (Hecht, 1998):

$$n_{21} = \frac{v_1}{v_2} \,, \tag{2.2.2}$$

where n_{21} is the refractive index of medium 2 with respect to the refractive index of medium 1, and v_1 and v_2 are speed of light in medium 1 and medium 2 respectively.

2.3 Fresnel Equation

The Fresnel equation explains the reflection and transmission of light when propagating to an interface between different optical media. We can calculated the relationship of the phase $\mathbf{E}_i(\mathbf{r},t)$, $\mathbf{E}_r(\mathbf{r},t)$ and $\mathbf{E}_t(\mathbf{r},t)$ which are exists at the boundary. First we determined the amplitude of $\mathbf{E}_{0i}$, $\mathbf{E}_{0r}$, and $\mathbf{E}_{0t}$ which are used to find the reflected and transmitted coefficient. We going to resolve its $\mathbf{E}_{i0}$ and $\mathbf{B}$ fields into components parallel and perpendicular to the plane of incidence, and treat these constituents separately (Peatross and Ware, 2015). Figure 2.2 shows the incoming waves of the electric field normal to the plane of incidence and the magnetic field is parallel to the plane incidence.

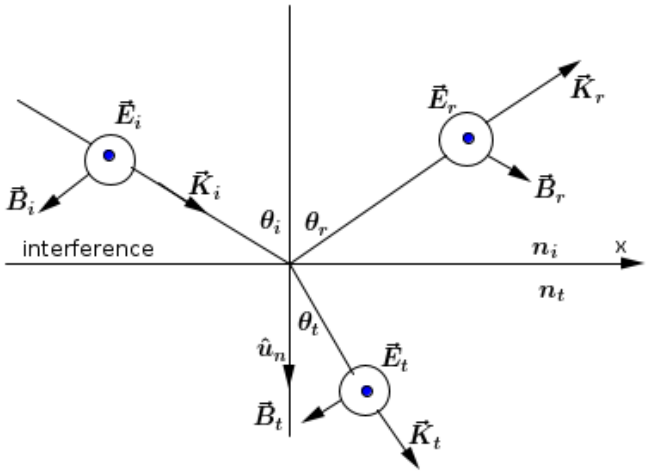

Figure 2.2: An incoming waves whose $\mathbf{E}$ field is normal to the plane of incidence (Hecht, 1998)

From Figure 2.2 we shall calculate the amplitude of the reflection coefficient and the amplitude of the transmission coefficient when the incident plane is perpendicular to the electric field. Finally, we

calculate the reflectance and transmittance intensity of this incident plane for the electric field. In this case the incident monochromatic light wave is planar , so that the electric field is given as

$$\mathbf{E}_i = \mathbf{E}_{0i} e^{i(\mathbf{k}_i.\mathbf{r}-\omega_i t)} . \tag{2.3.1}$$

When we simplify equation (2.3.1) it gives us

$$\mathbf{E}_i = \mathbf{E}_{0i} \cos(\mathbf{k}_i.\mathbf{r} - \omega_i t) . \tag{2.3.2}$$

Reflected and transmitted waves are given as

$$\mathbf{E}_r = \mathbf{E}_{0r} e^{i(\mathbf{k}_r.\mathbf{r}-\omega_r t+\epsilon_r)} \tag{2.3.3}$$
$$\mathbf{E}_t = \mathbf{E}_{0t} e^{i(\mathbf{k}_t.\mathbf{r}-\omega_t t+\epsilon_t)} . \tag{2.3.4}$$

To simplify equation (2.3.3) and equation (2.3.4) we write:

$$\mathbf{E}_r = \mathbf{E}_{0r} \cos(\mathbf{k}_r.\mathbf{r} - \omega_r t + \epsilon_r) , \tag{2.3.5}$$
$$\mathbf{E}_t = \mathbf{E}_{0t} \cos(\mathbf{k}_t.\mathbf{r} - \omega_t t + \epsilon_t) , \tag{2.3.6}$$

where ϵ_r and ϵ_t are phase constants .

From Figure 2.2 we have an electric field $\mathbf{E}$ is perpendicular to the incidence . Let us call E the magnitude of the electric field, where B is the magnetic field with $E = vB$.

$$\mathbf{K} \times \mathbf{E} = \mathbf{K} \times v\mathbf{B} = v\mathbf{B} ,$$

and we have

$$\mathbf{K}.\mathbf{E} = \mathbf{K}.v\mathbf{B} = 0 .$$

The tangential components of electric field $\mathbf{E}$ at any point is given as

$$\mathbf{E}_i + \mathbf{E}_r = \mathbf{E}_t . \tag{2.3.7}$$

Inserting equation (2.3.2), (2.3.5) and (2.3.6) into equation (2.3.7) we have

$$\mathbf{E}_{0i} \cos(\mathbf{k}_i.\mathbf{r} - \omega_i t) + \mathbf{E}_{0r} \cos(\mathbf{k}_r.\mathbf{r} - \omega_r t + \epsilon_r) = \mathbf{E}_{0t} \cos(\mathbf{k}_t.\mathbf{r} - \omega_t t + \epsilon_t) . \tag{2.3.8}$$

By cancelling the cosine and equation (2.3.8) can be given as

$$\mathbf{E}_{0i} + \mathbf{E}_{0r} = \mathbf{E}_{0t} \tag{2.3.9}$$

$$\mathbf{E}_{0r} = \mathbf{E}_{0t} - \mathbf{E}_{0i} \tag{2.3.10}$$

and

$$\mathbf{E}_{0i} = \mathbf{E}_{0t} - \mathbf{E}_{0r} . \tag{2.3.11}$$

The electric field $(\mathbf{E})$ and the magnetic field $(\mathbf{B})$ are explain as $\mathbf{E} = \epsilon\mathbf{E}$ and $\mathbf{B} = \dfrac{\mathbf{B}}{\mu}$ respectively.

Thus the tangential components of $\dfrac{\mathbf{B}}{\mu}$ is explained as

$$-\frac{\mathbf{B}_i}{\mu_i}\cos\theta_i + \frac{\mathbf{B}_r}{\mu_r}\cos\theta_r \quad = \quad -\frac{\mathbf{B}_t}{\mu_t}\cos\theta_t\,. \tag{2.3.12}$$

But we know that $\mathbf{E} = v\mathbf{B} \implies \mathbf{B_i} = \dfrac{\mathbf{E_i}}{v_i}, \mathbf{B_r} = \dfrac{\mathbf{E_r}}{v_r}$ and $\mathbf{B_t} = \dfrac{\mathbf{E_t}}{v_t}$.

Then equation (2.3.12) can be written as

$$\frac{\mathbf{E_i}}{v_i\mu_i}\cos\theta_i - \frac{\mathbf{E_r}}{v_r\mu_r}\cos\theta_r \quad = \quad \frac{\mathbf{E_t}}{v_t\mu_t}\cos\theta_t\,. \tag{2.3.13}$$

From the law of reflection we have $\theta_i = \theta_r$, and $v_i = v_r$, then equation (2.3.13) can be written as

$$\frac{(\mathbf{E_i} - \mathbf{E_r})}{v_i\mu_i}\cos\theta_i \quad = \quad \frac{\mathbf{E_t}}{v_t\mu_t}\cos\theta_t\,. \tag{2.3.14}$$

Let $\dfrac{C}{v_i} = n_i$ and $\dfrac{C}{v_t} = n_t$ and equation (2.3.14) can be rewritten as

$$\frac{n_i}{\mu_i}(\mathbf{E_{0i}} - \mathbf{E_{0r}})\cos\theta_i \quad = \quad \frac{n_t}{\mu_t}\mathbf{E_{0t}}\cos\theta_t\,. \tag{2.3.15}$$

First we calculate the amplitude of the reflection coefficient by inserting equation(2.3.9) into equation(2.3.15) :

$$\begin{aligned}
\frac{n_i}{\mu_i}(\mathbf{E_{0i}} - \mathbf{E_{0r}})\cos\theta_i &= \frac{n_t}{\mu_t}(\mathbf{E_{0i}} + \mathbf{E_{0r}})\cos\theta_t \\
\frac{n_i}{\mu_i}\mathbf{E_{0i}}\cos\theta_i - \frac{n_i}{\mu_i}\mathbf{E_{0r}}\cos\theta_i &= \frac{n_t}{\mu_t}\mathbf{E_{0i}}\cos\theta_t + \frac{n_t}{\mu_t}\mathbf{E_{0r}}\cos\theta_t \\
\frac{n_i}{\mu_i}\mathbf{E_{0i}}\cos\theta_i - \frac{n_t}{\mu_t}\mathbf{E_{0i}}\cos\theta_t &= \frac{n_i}{\mu_i}\mathbf{E_{0r}}\cos\theta_i + \frac{n_t}{\mu_t}\mathbf{E_{0r}}\cos\theta_t \\
\left(\frac{n_i}{\mu_i}\cos\theta_i - \frac{n_t}{\mu_t}\cos\theta_t\right)\mathbf{E_{0i}} &= \left(\frac{n_i}{\mu_i}\cos\theta_i + \frac{n_t}{\mu_t}\cos\theta_t\right)\mathbf{E_{0r}} \\
\implies \left(\frac{\mathbf{E_{0r}}}{\mathbf{E_{0i}}}\right)_\perp &= \frac{\dfrac{n_i}{\mu_i}\cos\theta_i - \dfrac{n_t}{\mu_t}\cos\theta_t}{\dfrac{n_i}{\mu_i}\cos\theta_i + \dfrac{n_t}{\mu_t}\cos\theta_t}\,.
\end{aligned} \tag{2.3.16}$$

Second, we calculate the amplitude of the transmission coefficient by inserting equation (2.3.10) into

equation (2.3.15) :

$$\begin{aligned}
\frac{n_i}{\mu_i}(\mathbf{E_{0i}} - (\mathbf{E_{0t}} - \mathbf{E_{0i}}))\cos\theta_i &= \frac{n_t}{\mu_t}\mathbf{E_{0t}}\cos\theta_t \\
\frac{n_i}{\mu_i}(\mathbf{2E_{0i}} - \mathbf{E_{0t}})\cos\theta_i &= \frac{n_t}{\mu_t}\mathbf{E_{0t}}\cos\theta_t \\
2\frac{n_i}{\mu_i}\mathbf{E_{0i}}\cos\theta_i - \frac{n_i}{\mu_i}\mathbf{E_{0t}}\cos\theta_i &= \frac{n_t}{\mu_t}\mathbf{E_{0t}}\cos\theta_t \\
2\frac{n_i}{\mu_i}\mathbf{E_{0i}}\cos\theta_i &= \frac{n_i}{\mu_i}\mathbf{E_{0t}}\cos\theta_i + \frac{n_t}{\mu_t}\mathbf{E_{0t}}\cos\theta_t \\
2\frac{n_i}{\mu_i}\cos\theta_i\mathbf{E_{0i}} &= \left(\frac{n_t}{\mu_t}\cos\theta_t + \frac{n_i}{\mu_i}\cos\theta_i\right)\mathbf{E_{0t}} \\
\implies \left(\frac{\mathbf{E_{0t}}}{\mathbf{E_{0i}}}\right)_\perp &= \frac{2\frac{n_i}{\mu_i}\cos\theta_i}{\frac{n_t}{\mu_t}\cos\theta_t + \frac{n_i}{\mu_i}\cos\theta_i}\,. \qquad (2.3.17)
\end{aligned}$$

The symbol $\perp$ denotes that $\mathbf{E}$ is perpendicular to the place of incidence .

Assume $\mu_i \approx \mu_t \approx \mu_0$ then equation (2.3.16) and equation (2.3.17) can be explained as

$$\begin{aligned}
r_\perp &= \left(\frac{\mathbf{E_{0r}}}{\mathbf{E_{0i}}}\right)_\perp \\
r_\perp &= \frac{n_i\cos\theta_i - n_t\cos\theta_t}{n_i\cos\theta_i + n_t\cos\theta_t}\,, \qquad (2.3.18)
\end{aligned}$$

and

$$\begin{aligned}
t_\perp &= \left(\frac{\mathbf{E_{0t}}}{\mathbf{E_{0i}}}\right)_\perp \\
t_\perp &= \frac{2n_i\cos\theta_i}{n_i\cos\theta_i + n_t\cos\theta_t}\,, \qquad (2.3.19)
\end{aligned}$$

where $r_\perp$ and $t_\perp$ are the amplitude of the reflection coefficient and the transmission coefficient respectively .

2.4 Reflectance and Transmittance Intensity

Power and intensity are directly related to each other. The incident power is given by

$$p_i = p_r + p_t\,. \qquad (2.4.1)$$

From equation (2.4.1) we have also that

$$p_i^{(s)} = p_r^{(s)} + p_t^{(s)}\,, \qquad (2.4.2)$$

and

$$p_i^{(p)} = p_r^{(p)} + p_t^{(p)}\,. \qquad (2.4.3)$$

Intensity is the square of the field amplitude and proportional to power, where reflectance is the fraction of the reflected power:

$$R_s = \frac{p_r^{(s)}}{p_i^{(s)}} = \frac{I_r^{(s)}}{I_i^{(s)}} = \frac{\left|E_{0r}^{(s)}\right|^2}{\left|E_{0i}^{(s)}\right|^2} = |r_s|^2 \,, \tag{2.4.4}$$

and

$$R_p = \frac{p_r^{(p)}}{p_i^{(p)}} = \frac{I_r^{(p)}}{I_i^{(p)}} = \frac{\left|E_{0t}^{(p)}\right|^2}{\left|E_{0i}^{(p)}\right|^2} = |r_p|^2 \,. \tag{2.4.5}$$

The total reflected intensity is given as

$$I_T = I_T^{(s)} + I_T^{(p)} = R_s I_i^{(s)} + R_p I_i^{(p)} \,. \tag{2.4.6}$$

The total incident intensity is given as

$$I_i = I_i^{(s)} + I_i^{(p)} = \frac{1}{2} n_i \epsilon_0 \left[\left|E_{0i}^{(s)}\right|^2 + \left|E_{0r}^{(p)}\right|^2\right] \,. \tag{2.4.7}$$

The total transmitted intensity is given as

$$I_t = I_t^{(s)} + I_t^{(p)} = \frac{1}{2} n_i \epsilon_0 \left[\left|E_{0t}^{(s)}\right|^2 + \left|E_{0t}^{(p)}\right|^2\right] \,. \tag{2.4.8}$$

2.5 Coherence

The coherence of a wave depend on the properties of its light source. If the two fields are non-coherent the interference at the detection point rapidly fluctuats between constructive and destructive interference, therefore the time averaged signal does not show interference (Peatross and Ware, 2015). The two classifications of coherence are temporal coherence and spatial coherence.

2.5.1 Temporal Coherence.

The correlation between the phase of a light wave at different points along the direction of the propagation is measured by temporal coherence. The characteristics and nature of monochromatic is measured by the temporal coherence. The equation of the temporal coherence function (autocorrelation) is given by

$$G(\tau) = \int_{-\infty}^{\infty} U^*(t) U(t+\tau) dt \,, \tag{2.5.1}$$

and

$$G^*(\tau) = \int_{-\infty}^{\infty} U(t) U^*(t-\tau) dt \,. \tag{2.5.2}$$

From equation (2.5.1) and equation (2.5.2) we have

$$G(-\tau) = G^*(\tau)\,. \tag{2.5.3}$$

The coherence length of a light source with a Gaussian emission spectrum is given by

$$L_c = t_c c = \sqrt{\frac{2\ln(2)}{\pi n}}\frac{\lambda^2}{\Delta\lambda}\,, \tag{2.5.4}$$

and the time for the coherence is given as

$$t = \frac{1}{\Delta\nu} = \frac{\lambda^2}{c\Delta\lambda}\,, \tag{2.5.5}$$

where $\Delta\nu$ is the spectral width of frequency, c is the speed of light , n is the refractive index of the medium, λ is the central wavelength and $\Delta\lambda$ is the full width half maximum (FWHM) of the emission peak in wavelength spectrum (Akcay et al., 2002).

2.5.2 Spatial Coherence.

Spatial coherence determines the uniformity of the phase of the wave front. Consider we have two slits at positions x_1 and x_2, and each wave front from slit left can be defined as complex values time dependent u and t. If the field that is emitted by the point source is monochromatic, the spacing between all the wave fronts are perfectly equal, so there is no random fluctuations. Therefore, let's assume that the light from the point source is not perfectly time harmonic, so that there is some slight variation in the distance between the wave fronts. Figure 2.3 shows the setup of double-slit experiments used to measure spatial coherence.

Let's describe the field that is emitted by the point source as a function of time U(t). If the time it takes for the wave fronts to reach the slit is respectively τ_1 and τ_2, then the fields at the slits are given by $U(t-\tau_1)$ and $U(t-\tau_2)$, where τ is given by the distance between the light source and the slit divided by the speed of light . If the distance from the source to the slits are the same then the field at the two slits are the same, so their fluctuations are perfectly correlated:

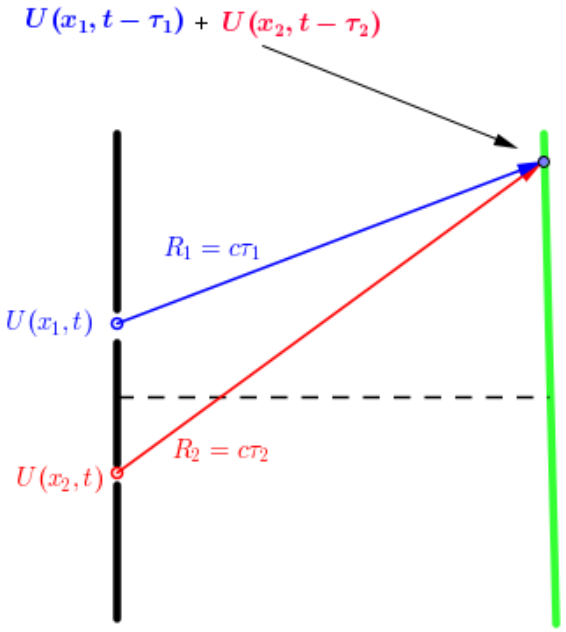

Figure 2.3: Double slits interference fringes

$$\begin{aligned} U(x_1,t) &= U_1 e^{-i\omega t}\,, \\ U(x_2,t) &= U_2 e^{-i\omega t}\,. \end{aligned} \tag{2.5.6}$$

The intensity will be measured as

$$\begin{aligned} I &= \langle |U(x_1, t-\tau_1) + U(x_2, t-\tau_2)|^2 \rangle \\ &= \langle \left| U_1 e^{-i\omega(t-\tau_1)} + U_2 e^{-i\omega(t-\tau_2)} \right|^2 \rangle \\ &= \langle |U_1|^2 + |U_2|^2 + U_1 U_2^* e^{-i\omega(\tau_2-\tau_1)} + U_1^* U_2 e^{i\omega(\tau_2-\tau_1)} \rangle \\ &= |U_1|^2 + |U_2|^2 + 2Re U_1 U_2^* e^{-i\omega(\tau_2-\tau_1)} \\ &= 2(1+\cos(\omega\tau+\phi))\,, \end{aligned} \tag{2.5.7}$$

where $U_1 = 1$, $U_2 = e^{i\phi}$ and $\tau = \tau_2 - \tau_1$.

3. Principle of Optical Coherence Tomography

OCT has special characteristics, like it is noninvasive and is non-destructive. OCT is used to identify very small structures, and it used to look under the skin. It can also be used to give information by producing a 3-dimensional image.

3.1 Interferences

A Young's double slit experiment is the famous demonstration of optical interference, and describes that the light from a single source radiate through two slits (or hole) can interfere to project an alternating fringe pattern of bright and dark bands on a screen. These bright and dark fringes occur because of the constructive and destructive interferences of light respectively. Depending on this bright and dark pattern the light waves from the two slits are inphase and add together up to a resultant maximum amplitude is called constructive interference, or when the light waves from the two slits are outphase we subtract up to a resultant minimum amplitude which called destructive interference. That these two (constructive and destructive interference) exist are based on the optical pathlength difference (OPD) between the slits to the same location on the screen (Peatross and Ware, 2015).

3.2 Michelson Interferometer

The principle of optical coherence tomography originates with the Michelson interferometer, which was invented by A.A.Michelson in 1881. OCT is analogous to ultrasound,as they measure the back reflection intensity of infrared light beams instead of using the echoes of sound. The back reflection intensity of OCT can not be measured electronically because of the high speed which is associated with the propagation of light (Strathman et al., 2013).

Figure 3.1 shows a Michelson interferometer, which consists of two reflective mirrors, mirror 1 and mirror 2. Light is emitted from the light source, hits the beam splitter, with half of the light going along path L_1 and reflected back to the beam splitter while the other half goes along optical path L_2 and is reflected back to the beam splitter (Strathman et al., 2013). These two light waves will interact with each other and be detected by the photodetector. Depending on the length difference between optical path L_1 and L_2, either constructive or destructive interference will occur. Since both return beams will go through the beam splitter (a half silvered mirror) again, they lose 50 $\%$ of their intensity. In some more complicated setups, a polarizing beam splitter (half silvered mirror) and wave retarders can be used to avoid this power lost.

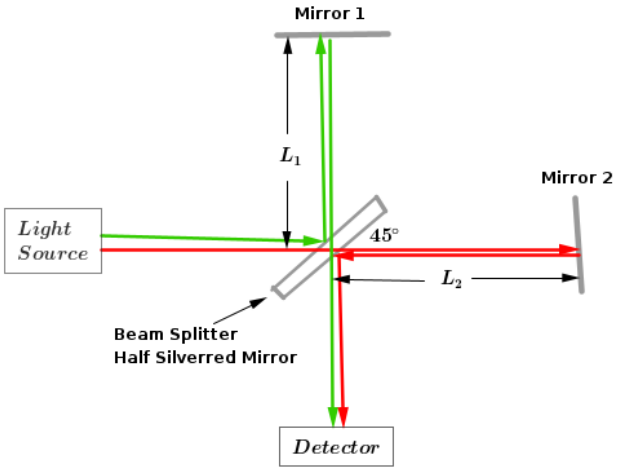

Figure 3.1: Schematic of the Michelson interferometer

Consider incident light as a plane wave, where the net field at the photodetector, which is the electric field coming from L_1 of the interferometer $\mathbf{E}(t,\tau) = \mathbf{E}_0 e^{i\omega(t+\tau)}$ and the electric field coming from L_2 is $\mathbf{E}(t) = \mathbf{E}_0 e^{i\omega t}$. The relationship between the time delay and the path difference is $\tau = \frac{d}{c}$. The two electric fields are the same except for the time delay τ. The total electric field is given as

$$\begin{aligned}\mathbf{E} &= \mathbf{E}(t,\tau) + \mathbf{E}(t) \\ &= \mathbf{E}_0 e^{i\omega(t+\tau)} + \mathbf{E}_0 e^{i\omega t} \\ &= \mathbf{E}_0 \left(e^{i\omega(t+\tau)} + e^{i\omega t}\right) \\ &= \mathbf{E}_0 e^{i\omega t}\left(e^{i\omega\tau} + 1\right) . \end{aligned} \tag{3.2.1}$$

The intensity is given as

$$\begin{aligned} I(\tau) &= \frac{nc\epsilon_0}{2} \left|\mathbf{E}(t,\tau) + \mathbf{E}(t)\right|^2 \\ &= \frac{nc\epsilon_0}{2} \left(\mathbf{E}_0 e^{i\omega(t+\tau)} + \mathbf{E}_0 e^{i\omega t}\right) . \left(\mathbf{E}_0 e^{i\omega(t+\tau)} + \mathbf{E}_0 e^{i\omega t}\right)^* \\ &= \frac{nc\epsilon_0}{2} \left(\mathbf{E}_0 e^{i\omega(t+\tau)} + \mathbf{E}_0 e^{i\omega t}\right) . \left(\mathbf{E}_0^* e^{-i\omega(t+\tau)} + \mathbf{E}_0^* e^{-i\omega t}\right) \\ &= \frac{nc\epsilon_0}{2} \mathbf{E}_0\mathbf{E}_0^* \left(e^{i\omega(t+\tau)} + e^{i\omega t}\right) . \left(e^{-i\omega(t+\tau)} + e^{-i\omega t}\right) \\ &= \frac{nc\epsilon_0}{2} \mathbf{E}_0\mathbf{E}^* \left(2 + e^{i\omega\tau} + e^{-i\omega\tau}\right) \\ &= \mathbf{E}_0\mathbf{E}^* \left(2 + 2\cos\left(\omega\tau\right)\right) \\ &= 2\mathbf{E}_0\mathbf{E}_0^* \left(1 + \cos\left(\omega\tau\right)\right) \\ I(\tau) &= 2I_0 \left(1 + \cos\left(\omega\tau\right)\right) , \end{aligned} \tag{3.2.2}$$

where $I_0 = \frac{nc\epsilon_0}{2}\mathbf{E}_0\mathbf{E}_0^*$.

But the intensity is a function of t and τ, which is $I(t,\tau)$ gives as

$$\begin{aligned} I(t,\tau) &= I(t) + I(t+\tau) + \frac{nc\epsilon_0}{2}\left[\mathbf{E}^*(t)\mathbf{E}(t+\tau) + \mathbf{E}(t)\mathbf{E}^*(t+\tau)\right] \\ &= I(t) + I(t+\tau) + nc\epsilon_0 Re\{\mathbf{E}(t)\mathbf{E}^*(t+\tau)\}\,. \end{aligned} \tag{3.2.3}$$

The signal intensity of equation (3.2.3) is

$$\begin{aligned} Sig(\tau) &= \int_{-\infty}^{\infty} I(t,\tau)dt \\ &= \int_{-\infty}^{\infty} \left(I(t) + I(t+\tau) + nc\epsilon_0 Re\{\mathbf{E}(t)\mathbf{E}^*(t+\tau)\}\right) dt \\ &= \int_{-\infty}^{\infty} I(t)dt + \int_{-\infty}^{\infty} I(t+\tau)dt + \int_{-\infty}^{\infty} nc\epsilon_0 Re\{\mathbf{E}(t)\mathbf{E}^*(t+\tau)\}dt\,. \end{aligned} \tag{3.2.4}$$

Now let us consider

$$\epsilon \equiv \int_{-\infty}^{\infty} I(t)dt = \int_{-\infty}^{\infty} I(t+\tau)dt \tag{3.2.5}$$

and

$$\int_{-\infty}^{\infty} \mathbf{E}(t)\mathbf{E}^*(t+\tau)dt = \frac{1}{\sqrt{2\pi}}\int_{-\infty}^{\infty} d\omega e^{-i\omega\tau}\left[\frac{1}{\sqrt{2\pi}}\int_{-\infty}^{\infty} d\tau e^{i\omega\tau}\int_{-\infty}^{\infty} \mathbf{E}(t)\mathbf{E}^*(t+\tau)dt\right]. \tag{3.2.6}$$

Then inserting equation (3.2.5) and (3.2.6) into equation (3.2.4) we have

$$\begin{aligned} Sig(\tau) &= 2\epsilon\left[1 + \frac{1}{\epsilon}Re\int_{-\infty}^{\infty} I(\omega)e^{-i\omega\tau}d\omega\right] \\ &= 2\epsilon\left[1 + Re\{\gamma(\tau)\}\right]\,. \end{aligned} \tag{3.2.7}$$

But we have

$$\gamma(\tau) = \frac{\int_{-\infty}^{\infty} I(\omega)e^{-i\omega\tau}d\omega}{\int_{-\infty}^{\infty} I(\omega)d\omega}\,. \tag{3.2.8}$$

Let assume the $I(\omega)$ of the pulse in Gaussian and is given as

$$\begin{aligned} I(\omega) &= \frac{nc\epsilon_0}{2}E_0E_0^*T^2e^{-T^2(\omega-\omega_0)^2} \\ \int_{-\infty}^{\infty} I(\omega)d\omega &= \frac{nc\epsilon_0}{2}E_0E_0^*T\sqrt{\pi}\,. \end{aligned} \tag{3.2.9}$$

Now the degree of coherence from equation (3.2.8) becomes

$$\begin{aligned} \gamma(\tau) &= \frac{1}{\sqrt{\pi}}\int_{-\infty}^{\infty} e^{-T^2(\omega-\omega_0)^2}e^{-i\omega\tau}d\omega \\ &= \frac{T}{\sqrt{\pi}}\sqrt{\frac{\pi}{T^2}}e^{\frac{(2T^2\omega_0 - i\tau)^2}{4T^2} - T^2\omega_0^2} \\ \gamma(\tau) &= e^{-\tau^2/4T^2}e^{-i\omega_0\tau}\,. \end{aligned} \tag{3.2.10}$$

Then inserting equation (3.2.10) into equation (3.2.7) and the signal intensity is given as

$$Sig(\tau) = 2\epsilon \left(1 + e^{-\tau^2/4T^2} \cos(\omega_0 \tau)\right) . \tag{3.2.11}$$

OCT is a modern instrument which is used to produce an image, and image technology projects a light beam (820 nm) near the infrared wavelength. Figure 3.2 shows the setup of OCT, with they are almost Michelson interferometer setup. In this setup only one reference mirror (a movable mirror) is used and another reference mirror is replaced by a sample of glass. The beam from the light source is split into two by the beam splitter. The probe beam reaches the sample, and the reference beam reaches the reference mirror at a known distance. The echo time or delay of the light reflected from the various layers of the sample, is compared with the echo time delay of light reflected from the reference mirror. A positive interference is produced when light reflected from the sample and reference mirror arrives simultaneously. The interferometer integrates several data points over a 2mm depth to construct a tomogram of retinal structures (Strathman et al., 2013).

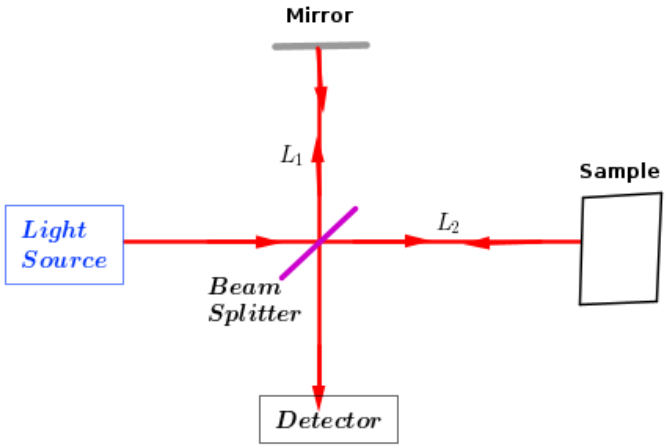

Figure 3.2: Schematic of OCT in Michelson interferometer

From figure 3.2 we have an incidence electric field, coefficient of reflection and transmission of a glass sample. Let us derive the equation of the incident electric field of sample and calculate the intensity at the detector. Consider the incident light as a plane wave, where the net field at the photodetector includes the electric field coming from L_1 of the interferometer $\mathbf{E}_0(t,\tau) = \mathbf{E}e^{i\omega(t+\tau)}$, and the electric field coming from L_2 as $\mathbf{E}_0(t) = \mathbf{E}e^{i\omega t}$.

Therefore, the electric field of the sample is given as

$$\begin{aligned}
\mathbf{E}_s &= r_{12}\mathbf{E}_0 + r_{21}t_{12}t_{21}\mathbf{E}_0\left(t+\frac{2dn}{c}\right)+... \\
&= r_{12}\mathbf{E}_0 + r_{12}t_{12}t_{12}\mathbf{E}_0\left(t+\frac{2dn}{c}\right)+... \\
&= r_{12}\mathbf{E}_0 + r_{12}t_{12}^2\mathbf{E}_0\left(t+\frac{2dn}{c}\right)+... \\
&= r_{12}\mathbf{E}_0\left(\frac{1}{1-t_{12}^2e^{i\omega\sigma}}\right) \\
&= \mathbf{E}_0\left(\frac{\sqrt{1-t_{12}^2}}{1-t_{12}^2e^{i\omega\sigma}}\right) \\
&= \mathbf{E}_0\left(\frac{r_{12}}{1-t_{12}^2e^{i\omega\sigma}}\right) \\
\mathbf{E}_s &= \mathbf{E}_0 r_s\,, \qquad (3.2.12)
\end{aligned}$$

where $r_{12}=-r_{21}$, $t_{12}=-t_{21}$,$r_s=\dfrac{r_{12}}{1-t_{12}^2e^{i\omega\sigma}}$, $\sigma=\dfrac{2nd}{c}$, and $r_{12}=\sqrt{1-t_{12}^2}$.

From equation (2.3.18) we have

$$r_{12}=\frac{n_1\cos\theta_i-n_2\cos\theta_t}{n_1\cos\theta_i+n_2\cos\theta_t}\,. \qquad (3.2.13)$$

By using Snell's law to write the angle of transmittance θ_t in terms of the incident angle θ_i equation (3.2.13) can be given as

$$r_{12}=\frac{n_1\cos\theta_i-n_2\sqrt{1-\left(\dfrac{n_1}{n_2}\sin\theta_i\right)^2}}{n_1\cos\theta_i+n_2\sqrt{1-\left(\dfrac{n_1}{n_2}\sin\theta_i\right)^2}}\,. \qquad (3.2.14)$$

And from equation (2.3.19) we have

$$t_{12}=\frac{2n_1\cos\theta_i}{n_1\cos\theta_i+n_2\cos\theta_t}. \qquad (3.2.15)$$

By using Snell's law equation (3.2.15) can be written as

$$t_{12}=\frac{2n_1\cos\theta_i}{n_1\cos\theta_i+n_2\sqrt{1-\left(\dfrac{n_1}{n_2}\sin\theta_i\right)^2}}\,. \qquad (3.2.16)$$

The electric field coming from the reference mirror is given as

$$E_0(t,\tau)=Ee^{i\omega(t+\tau)}\,. \qquad (3.2.17)$$

The total electric field E_T at the detector is the vector addition of the electric field coming from the sample and mirror. Hence the total electric field is calculated as

$$
\begin{aligned}
E_T &= E_0(t+\tau) + E_s(t) \\
&= Ae^{-t^2/\tau_p^2} e^{i\omega t} \left(e^{i\omega\tau} + r_{12} \left(\frac{1}{1 - t_{12}^2 e^{i\omega \frac{2nd}{c}}} \right) \right) \\
&= Ae^{-t^2/\tau_p^2} e^{i\omega t} \left(e^{i\omega\tau} + \frac{r_{12}}{1 - t_{12}^2 e^{i\omega 2nd/c}} \right) \\
E_T &= Ae^{-t^2/\tau_p^2} e^{i\omega t} \left(e^{i\omega\tau} + r_s \right) , \qquad (3.2.18)
\end{aligned}
$$

where $E = Ae^{-t^2/\tau_p^2}$.

The total intensity as a function of t and τ is derived as

$$
\begin{aligned}
I(t,\tau) &= \frac{nc\epsilon_0}{2} \left| E_0(t+\tau) + E_s(t) \right|^2 \\
&= \frac{nc\epsilon_0}{2} \left(E_0(t+\tau) + E_s(t) \right) . \left(E_0(t+\tau) + E_s(t) \right)^* \\
&= \frac{nc\epsilon_0}{2} \left[E_0(t+\tau) E_0(t+\tau)^* + E_s(t) E_s(t)^* + E_0(t+\tau)^* E_s(t) + E_0(t+\tau)^* E_s(t) \right] \\
&= I(t+\tau) + I_s(t) + \frac{nc\epsilon_0}{2} \left[E_0(t+\tau)^* E_s(t) + E_0(t+\tau)^* E_s(t) \right] \\
I(t,\tau) &= I(t+\tau) + I_s(t) + \frac{nc\epsilon_0}{2} Re\{ E_0(t+\tau)^* E_s(t) \} . \qquad (3.2.19)
\end{aligned}
$$

Using the same procedure as with the Michelson interferometer, the signal intensity is given as

$$
\begin{aligned}
Sig(\tau) &= \int_{-\infty}^{\infty} I(t,\tau) dt \\
&= \int_{-\infty}^{\infty} \left(I(t+\tau) + I_s(t) + \frac{nc\epsilon_0}{2} Re\{ E_0(t+\tau)^* E_s(t) \} \right) dt \\
Sig(\tau) &= \int_{-\infty}^{\infty} (I(t+\tau) dt + \int_{-\infty}^{\infty} I_s(t) dt + \int_{-\infty}^{\infty} \frac{nc\epsilon_0}{2} Re\{ E_0(t+\tau)^* E_s(t) \} dt . \qquad (3.2.20)
\end{aligned}
$$

Therefore, the total signal intensity of the OCT in a Michelson interferometer setup is given as

$$
Sig(\tau) = I_0 \left(R_r + \sum_{n=1}^{\infty} R_s + \sum_{n=1}^{\infty} \sqrt{R_r R_s} e^{\frac{-\tau^2}{4T^2}} \cos(\omega_0 \tau) \right) , \qquad (3.2.21)
$$

where R_r and R_s are the reflective of reference mirror and sample glass respectively.

3.3 Time Domain OCT

Time domain OCT (TD-OCT) focuses on the basic principles of white light interferometry. In Michelson interferometry, back scattered light from the sample glass is superimposed with light from a reference

beam, which is obtained with the beam splitter and the pathlength from the source to a sample glass. Only light from a selected small depth range can contribute to an oscillatory signal since only that light has a substantial temporal coherence with the reference beam.

In TD-OCT the optical path difference of the reference mirror is changed within a time interval. This time domain OCT also used low coherence interference. When the path difference at the detector in the same time makes a bright fringe, this is called constructive interference , and for dark fringes, it is destructive interference. The interference of the two partial coherent lights beam will be explained in terms of intensity I_s as

$$I = r_1 I_s + r_2 I_s + 2\sqrt{r_1 I_s . r_2 I_s} Re[\gamma(\tau)] \,, \tag{3.3.1}$$

where $r_1 + r_2 < 1$ is the interferometer beam splitter ratio and $\gamma(\tau)$ represents the complex degree of coherence . Because of the coherence gating effect the complex degree of coherence is given by a Gaussian envelope . The equation of the complex degree of coherence is given as

$$\gamma(\tau) = exp\Big[- \left(\frac{\pi \Delta\nu \tau}{2\sqrt{\ln 2}} \right)^2 \Big] exp(-j2\pi\nu_0\tau) \,, \tag{3.3.2}$$

where $\Delta\nu$ is the spectral width of the optical frequency domain, and ν_0 is the central optical frequency of the source (de Boer et al., 1998) .

3.4 Spectral Domain OCT

Another name of Fourier domain OCT is spectral domain OCT,where instead of recording not only the overall back-scattered optical power , one records the whole optical spectra of light , using some kind of spectrograph . For example, one may spatially disperse the light at a diffraction grating before sending it to a linear photodetector array . Essentially , one can consider each optical wavelength to provide information about the variation of optical properties of the sample with a certain spatial period. The spatial dependence can then be retrieved by applying a Fourier transform (Huang et al., 1991) .

The most effective spectral domain OCT is a measurement without using a scanning delay . Spectral domain OCT can be faster , because it does not use any moving components . Spectral domain OCT may be more sensitivity when compared with the time domain OCT .

3.5 Fourier Transform

Both frequency series and Fourier transforms are the mathematical tools for representing signals in the frequency domain. The only difference is , Fourier series are mainly used for periodic signals where as a Fourier transform is used for aperiodic signals . The Fourier transform in real cases of cosine-sine is given as

$$a[x] = \frac{2}{p} \int_0^p f(t) \cos\left(\frac{2\pi x t}{p} \right) dt \tag{3.5.1}$$

and

$$b[x] = \frac{2}{p} \int_0^p f(t) \sin\left(\frac{2\pi x t}{p} \right) dt \,. \tag{3.5.2}$$

The synthesis equation of this Fourier transform

$$f(t) = \frac{a[0]}{2} + \sum_{x=0}^{\infty} \left(a[x] \cos\left(\frac{2\pi x t}{p}\right) + b[x] \sin\left(\frac{2\pi x t}{p}\right) \right) . \tag{3.5.3}$$

The equation of the Gaussian normal distribution is given as

$$g(t) = \frac{1}{\sqrt{2\pi\sigma^2}} exp\left(-\frac{1}{2} \left(\frac{t}{\sigma}\right)^2 \right) . \tag{3.5.4}$$

The relationship between Fourier analysis G(f) and Gaussian distributions in equation (3.5.4) is given by

$$\begin{aligned}
G(f) &= \int_{-\infty}^{\infty} g(t) e^{-i2\pi f t} dt \\
&= \int_{-\infty}^{\infty} \frac{1}{\sqrt{2\pi\sigma^2}} e^{-\frac{1}{2}\left(\frac{t}{\sigma}\right)^2} e^{-i2\pi f t} dt \\
&= \frac{1}{\sqrt{2\pi\sigma^2}} \int_{-\infty}^{\infty} e^{-\frac{1}{2}\left(\frac{t}{\sigma}\right)^2} e^{-i2\pi f t} dt \\
&= \frac{1}{\sqrt{2\pi\sigma^2}} \int_{-\infty}^{\infty} e^{-\frac{1}{2}\left(\frac{t}{\sigma}\right)^2} \cos\left(-2\pi f t\right) dt \\
&= \frac{1}{\sqrt{2\pi\sigma^2}} \sqrt{2\pi\sigma^2} e^{-2\pi^2\sigma^2 f^2} \\
&= \frac{1}{\sqrt{2\pi\sigma^2}} \sqrt{2\pi\sigma^2} exp\left(-\frac{1}{2} \left(2\pi\sigma f\right)^2 \right) \\
G(f) &= exp\left(-\frac{1}{2} \left(2\pi\sigma f\right)^2 \right) .
\end{aligned} \tag{3.5.5}$$

4. Results and Discussion

In the previous chapter we have discussed the principles of OCT and the way OCT can be like a Michelson interferometer. However, in this chapter we review the analysis, discussion and the simulation of this essay project. The intensity of the Michelson interferometer was simulated, and the signal intensity of the Michelson interferometer in monochromatic and broadband sources was simulated. The signal intensity of OCT in a Michelson interferometer, when one reference mirror is replaced by a glass sample which has refractive index 1.5 and thickness 1mm using monochromatic and broadband source was simulated.

4.1 Simulations of Signal from Michelson Interferometer

We simulated the intensity with the function of time at a detector. In this simulation we used the central wavelength (λ_0) 1μm and the spectral width ($\Delta\lambda$) 100 nm for the light source and the velocity and position of the mirror as constant. This simulation is from equation (3.2.2). The intensity which exists at the detector in the Michelson interferometer, with an incident wave as a function of time, is shown in figure 4.1.

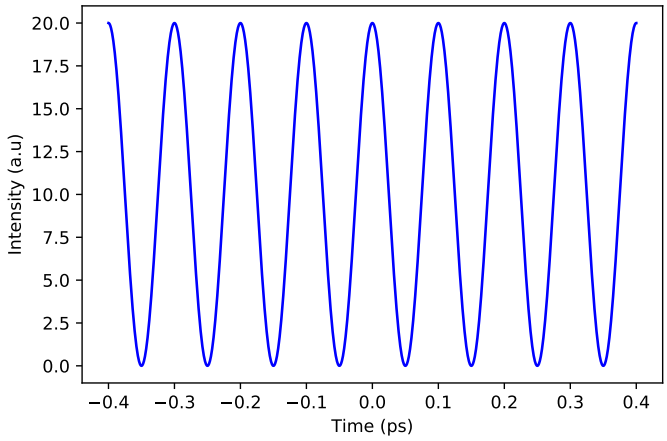

Figure 4.1: The intensity of Michelson interferometer

When the time was zero the maximum intensity existed and all the incident light are not occur.

We simulated the signal intensity of a monochromatic source, as shown in figure 4.2. The signal intensity of the monochromatic source was simulated where the horizontal axis shows the time difference between the movable mirror and the fixed mirror. This simulation of signal intensity of a monochromatic source is simulated from equation (3.2.3). In this simulation we used the central wavelength (λ_0) 1μm and the spectral width ($\Delta\lambda$) 100 nm of the light source, and the velocity and position of the mirror as constant.

The maximum amplitude is the constructive interfence as well as the minimum amplitude for the destructive interference. When the time difference is zero, the reflectance is maximum, and this is called constructive interference.

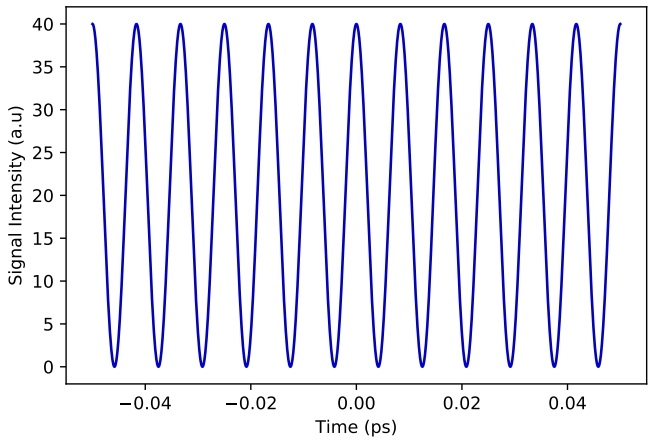

Figure 4.2: Signal intensity of a monochromatic source.

We simulated the signal intensity of the Michelson interferometer using a broadband coherent source, as shown in figure 4.3. This simulation of signal intensity has a Gaussian envelope as in equation (3.2.11). In this case we have some amount of continuous broadband sources, and we used the central wavelength (λ_0) 1μm and the spectral width ($\Delta\lambda$) 100 nm of the light source, and where velocity and position of the mirror were constant. For this signal intensity the movable mirror is $1.5ps$. The horizontal axis shows the time difference of the movable mirror.

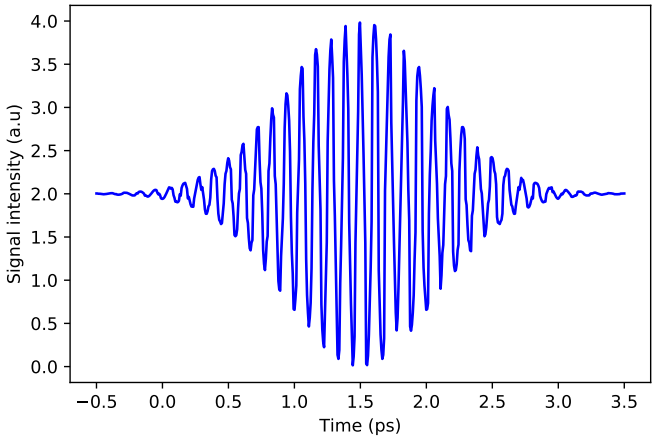

Figure 4.3: Signal intensity of broadband coherent source.

From this Michelson interferometer the signal intensity of light with a Gaussian spectrum as time is increased or decreased, the output signal intensity started to oscillated. In this case when we move the reference mirror by half length we get a different fringe pattern at each time.

4.2 Simulations of OCT in a Michelson Interferometer

We simulated signal intensity at the detector using a monochromatic source. In this case, we replaced one of the reference mirrors with a sample of glass. This sample glass has a thickness of 1 mm, and a refractive index of 1.5. From those setup we measure the reflection and transmission of the sample of glass as a function of time. First we calculated the electric field, where the Fresnel equations are of perpendicular incidence. That is, there would be a reflection at the first surface, off the second surface, and then also multiple reflections, which is called Fabry Perot reflections. The number of reflections we took into account would depend on the duration of the scan.

The signal intensity of OCT in a Michelson interferometer using a monochromatic source with a long coherence length as a function of time is shown in figure 4.4. The simulation of this signal intensity of OCT using a monochromatic source is simulated from equation (3.2.19). The maximum amplitude is for constructive interference,and the minimum amplitude is for destructive interference. When the time difference is zero the reflectance is maximum and it is called constructive interference. That means the monochromatic signal intensity fringes are inphase only for a time of zero.

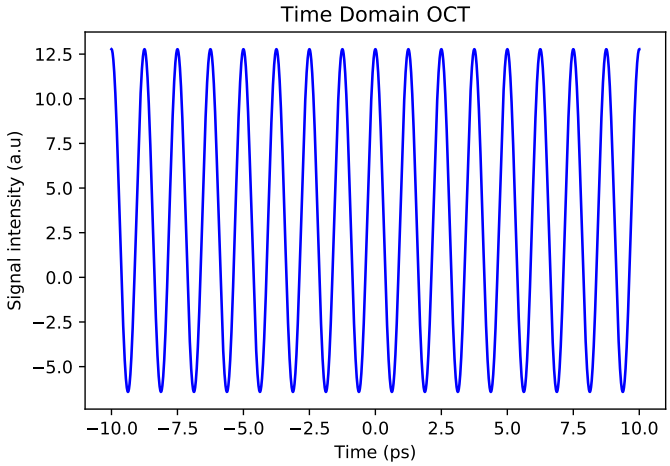

Figure 4.4: Signal intensity of monochromatic sources

Figure 4.5 shows the signal intensity of OCT in a Michelson interferometer using a broadband source. In this simulation we used the central wavelength of (λ_0) 1μm, and the spectral width ($\Delta\lambda$) of 100 nm for the light source and simulated from equation (3.2.21). Signal intensity for the optical path length of the sample glass and movable mirror was matched to within the narrow coherence length as the light source used low coherence (broadband sources).

The movable mirror started to scan when the optical path length of the reflections from within the sample glass was matched to each other. The incoming light source was split into two by the beam splitter. This means that when the incoming light passed through two different pathlengths L_1, and L_2 then were collinearly superimposed at the beam splitter, the two pulses reflected in each arm of the interferometer, and one of the arm's length is increased, the distance which causes a delay on recombining .

The sample glass, as detected by a photodetector as a function of the width of time auto-correlation$=\frac{2nd}{c}$ between the pulses, while the fundamental wavelength iwas rejected. Since the refractive index

and thickness of glass is 1.5 and $1mm$ respectively, based on this values we calculated a width of time $= 10$ pico seconds $(10ps)$ and frequency $1x10^{12}$ Hertz $(1THz)$. Thus the time width of this pulse in the time domain is given as

$$\begin{aligned} t_w &= \frac{2nd}{c} \\ t_w &= \frac{2 * 1.5 * 10^{-3}}{3 * 10^8} \\ t_w &= 10ps\,, \end{aligned}$$

where t_w is time width of the pulse.

We calculated the time delay at the detector using the width of the time pulse, where the central wavelength was (λ_0) 1μm, and the spectral width $(\Delta\lambda)$ was 100 nm , as

$$t = \frac{10^{-12}}{3 * 10^8 * 10^{-7}} = 3.3ps\,. \tag{4.2.1}$$

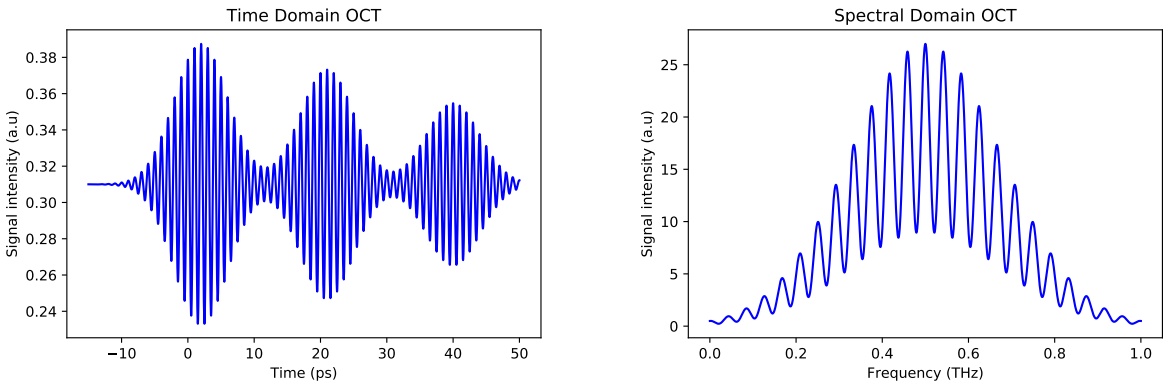

Figure 4.5: Signal intensity of a broadband coherent source.

In this time domain OCT three of these pulses have the same approximate width but different heights. In the simplest method we measured the shape of the pulse as changing with the distance of the time depth of the reference mirror, and then we could see the signal intensity of our sample glass. The time delay of the movable mirror in this signal intensity of OCT was twice the time delay of the movable mirror of the signal intensity of Michelson interferometry.

In the spectral domain of OCT, first we derived the total electric field of the reference mirror and sample glass in equation (3.2.18). Since we have the values of the refractive index of glass, 1.5, and the thickness of the glass, 1mm, we easily simulated the electric field. Additionally, we have some constant values, such as the reflection coefficient and transmission coefficient, as well as the values of the angular frequency (ω) and tau (τ) as also being constant. After we simulated the electric field we found the Fourier transform of this electric field. This Fourier transform of the electric field is the spectral domain of the OCT. We measured this spectral domain of the OCT without moving the mirror, and we used only focusing the Fourier transform of an electric field of a sample glass.

4.3 Fourier Transforms of Simulated Signals

Figure 4.6 shows the time domain and frequency domain of the Gaussian function. We simulated the time domain from equation (3.5.4) and the frequency domain from equation (3.5.5). In this case the values of $\sigma = 0.25$ and the bandwidth of the time domain become narrow. However, the same values of $\sigma = 0.25$ the bandwidth of the Fourier domain become wider. From this result we observe that the time domain is the inverse of the frequency domain.

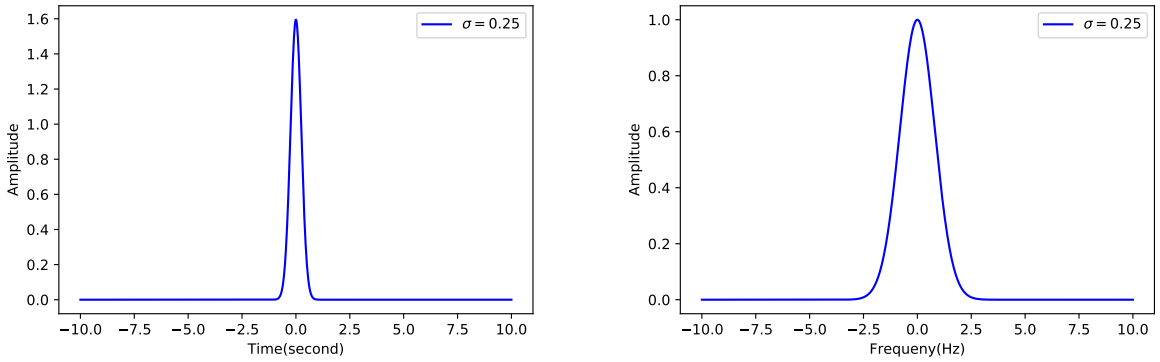

Figure 4.6: Fourier transform of the Gaussian

5. Conclusions and Future Work

5.1 Conclusions

In our work we have discussed the application of OCT in Michelson interferomter. We have seen that the most important part of a OCT is the time domain and spectral domain. The time domain is based on a moving mirror, but the spectral domain is not based on this moving mirror, it is based on the Fourier transform of an electric field. OCT has many applications in hospitals and industry, but it is most by used of on transparent materials or tissue. OCT is a modern technique which is used to create two or three dimensional images without to involving any ionizing radiation. The way we measured the signal intensity at the detector in OCT is the same method as for the Michelson interferometer, however we replaced with a sample of glass the fixed mirror.

We then talked about the time domain and spectral domain using a broadband source, and a sample glass instead of a reference mirror on one side. We have show that, from our results and simulation, that the time domain generates ultrafast laser pulses in the range of picoseconds. We computed some of the characteristics of the pulses, such as their ultrafast laser pulse duration (ps), repetition time and intensity signal. As our results show the numerical simulation of using the auto-correlaton function to determine the temporal size of ultrafast pulse durations is $10ps$ in the time domain of OCT. So, we conclude that from our discussion and analysis, the time domain is one of the best techniques for generating ultrafast laser pulses.

5.2 Future Work

In this project there are many directions for future work, where we could verify these theoretical values with the experimental results using the spectrometer or photo-detector in the laboratory working . We can also determine the time domain and spectral domain in the OCT using experimental in laboratory working. We could use clinical and hospital data by scanning the retina, and to study the diseases of the eye by using this OCT in a laboratory.

Acknowledgements

First of all, I would like to thank almighty God, who gave me the chance to successfully accomplish my studies. Next, I would like to thank my supervisors: Dr. Pieter Neethling and Dr. Gurthwin Bosman, for their constructive comments, guidance and endless support from the beginning to the end of my studies in the program at the African Institute for Mathematical Sciences (AIMS). I respectfully thank AIMS and the University of Stellenbosch for giving me the opportunity to study a structured masters. Finally, I would like to express my thanks from the bottom of my heart, to all my family members and my tutors and instructors at AIMS. My special thanks goes to my mother, Gurale Geleta, and my wife, Hana Bedasa, for their love, and continuous support. Last but not least, my heartfelt gratitude goes to my fellow friends and colleagues. They deserve special thanks for their valuable contributions and encouragement.

References

Akcay, C., Parrein, P., and Rolland, J. P. Estimation of longitudinal resolution in optical coherence imaging. *Applied optics*, 41(25):5256–5262, 2002.

de Boer, J. F., Milner, T. E., van Gemert, M. J., and Nelson, J. S. Two-dimensional birefringence imaging in biological tissue using phase and polarization sensitive optical coherence tomography. In *Advances in Optical Imaging and Photon Migration*, page AMC2. Optical Society of America, 1998.

Fujimoto, J. G., Pitris, C., Boppart, S. A., and Brezinski, M. E. Optical coherence tomography: an emerging technology for biomedical imaging and optical biopsy. *Neoplasia (New York, NY)*, 2(1-2): 9, 2000.

Hecht, E. Optics 4th edition. optics. *Addison Wesley Longman Inc*, 1:1998, 1998.

Huang, D., Swanson, E. A., Lin, C. P., Schuman, J. S., Stinson, W. G., Chang, W., Hee, M. R., Flotte, T., Gregory, K., Puliafito, C. A., et al. Optical coherence tomography. *Science*, 254(5035):1178–1181, 1991.

Peatross, J. and Ware, M. Physics of light and optics 2015 edition http://optics.byu.edu, 2015.

Pircher, M., Götzinger, E., Leitgeb, R., Fercher, A. F., and Hitzenberger, C. K. Measurement and imaging of water concentration in human cornea with differential absorption optical coherence tomography. *Optics Express*, 11(18):2190–2197, 2003.

Schmitt, J. M. Optical coherence tomography (oct): a review. *IEEE Journal of selected topics in quantum electronics*, 5(4):1205–1215, 1999.

Strathman, M., Liu, Y., Li, X., and Lin, L. Y. Dynamic focus-tracking mems scanning micromirror with low actuation voltages for endoscopic imaging. *Optics express*, 21(20):23934–23941, 2013.

Youngquist, R. C., Carr, S., and Davies, D. E. Optical coherence-domain reflectometry: a new optical evaluation technique. *Optics letters*, 12(3):158–160, 1987.